Are your MRI contrast agents cost-effective?
Learn more about generic Gadolinium-Based Contrast Agents.
FRESENIUS KABI
caring for life

AJNR

Fast inversion-recovery MR: the effect of hybrid RARE readout on the null points of fat and cerebrospinal fluid.

E R Melhem, H Jara, H Shakir and T A Gagliano

AJNR Am J Neuroradiol 1997, 18 (9) 1627-1633
http://www.ajnr.org/content/18/9/1627

This information is current as of April 19, 2024.

Fast Inversion-Recovery MR: The Effect of Hybrid RARE Readout on the Null Points of Fat and Cerebrospinal Fluid

Elias R. Melhem, Hernan Jara, Huzeifa Shakir, and Todd A. Gagliano

PURPOSE: To evaluate the effect of the hybrid RARE (rapid acquisition with relaxation enhancement) readout, commonly coupled to inversion-recovery pulse sequences, on the null inversiton time (TI) of fluid and fat using both phantoms and human volunteers. **METHODS:** Two phantoms, simulating fat (phantom A) and cerebrospinal fluid (phantom B), respectively, were imaged using a fast inversion-recovery sequence that coupled an inversion-recovery preparation pulse to a hybrid RARE readout. At repetition times (TRs) ranging from 700 to 20 000, the TI necessary to null the signal from each phantom (null TI) was determined for an echo train length of 4, 6, 8, 10, 12, 14, 16, 18, and 20, respectively. Plots of null TI versus echo train length at different TRs were generated for both phantoms. Fast inversion-recovery MR imaging of the cervical spine and brain was performed in healthy volunteers. At a fixed TR and TI, the adequacy of signal suppression from bone marrow and cerebrospinal fluid was assessed as a function of echo train length. **RESULTS:** There was a gradual decrease of null TI for both phantoms with echo train length. This decrease persisted at longer TRs for phantom B (T1 = 3175 ± 70 milliseconds) than for phantom A (T1 = 218 ± 5 milliseconds). In the human volunteers, there was a gradual loss of suppression of signal from bone marrow and cerebrospinal fluid, with changes in the hybrid RARE readout. **CONCLUSION:** To optimize specific tissue suppression, radiologists implementing fast inversion-recovery MR imaging should be aware of the effects of the hybrid RARE readout on null TI.

Index term: Magnetic resonance, technique

AJNR Am J Neuroradiol 18:1627–1633, October 1997

The clinical utility of selective tissue suppression using inversion-recovery pulse sequences has been documented extensively in the literature (1–8). Specific modifications of inversion time (TI) can lead to effective suppression of cerebrospinal fluid (CSF) in the central nervous system and of fat in the bone marrow and in the orbits (2, 4, 5). In the past, one of the major deterrents to the more common use of these inversion-recovery magnetic resonance (MR) imaging techniques has been the length of the acquisition time. Recently, imaging efficiency and clinical utility have been improved by incorporating technical refinements, including rapid acquisition with relaxation enhancement (RARE) and sequential interleaving (9–13).

The standard equation for determining the null TI (specific TI needed to cause selective suppression of signal from tissue *X* with a given T1 relaxation time) using a conventional spin-echo readout is

$$1) \quad \text{null TI}_x = \text{T1}_x[\ln 2 - \ln(1 + e^{-\text{TR}/\text{T1}x})](12).$$

It can be inferred from the above equation that the null TI of a specific tissue *X* when using conventional inversion-recovery pulse sequences is solely dependent on the T1 relaxation time of the tissue and on the selected repetition time (TR).

The purpose of this study was to evaluate the effect of the hybrid RARE readout on the null TI of water and fat phantoms, as well as to assess its effect on signal suppression in the clinical setting, using human volunteers.

Received January 30, 1997; accepted after revision April 8.

Supported in part by a research grant from Philips Medical Systems.

From the Department of Radiology, Boston University Medical Center, 88 E Newton St, Atrium 2, Boston, MA 02118. Address reprint requests to Elias R. Melhem, MD.

AJNR 18:1627–1633, Oct 1997 0195-6108/97/1809–1627

© American Society of Neuroradiology

Materials and Methods

All MR imaging was performed on two 1.5-T magnets with maximum gradients of 10 and 15 mT m^{-1}, and maximum slew rates of 10 and 17 mT m^{-1} ms^{-1}, respectively. MR images of the phantoms and brain were obtained with a standard quadrature head coil operating in receive mode. MR images of the cervical spine were obtained with a quadrature neck coil operating in receive mode.

Phantom Experiments

Two phantoms were used to simulate fat and CSF, respectively. Phantom A consisted of corn oil (T1/T2: 218 ± 5 milliseconds/47 ± 1 millisecond). Phantom B consisted of distilled water (T1/T2: 3175 ± 70 milliseconds/1786 ± 185 milliseconds). The T1 and T2 relaxation times of the two phantoms were measured according to the method described by In den Kleef and Cuppen (14).

Both phantoms were imaged using a fast inversion-recovery sequence that coupled an inversion-recovery preparation pulse to a hybrid RARE readout. The incorporated hybrid RARE readout implemented an echo-to-view mapping scheme that achieved the shortest possible effective echo times (TE_{eff}s). The lower-order phase-encoded lines were acquired at the beginning of the echo train, while the outer lines were acquired at later times in alternating fashion. In each shot, the successive profiles were closely packed, separated in time by an echo spacing equal in value to the TE_{eff}. This hybrid RARE readout allowed variation of the echo train length without altering the echo spacing.

The phantoms were imaged in the coronal plane using the following fixed parameters: TE_{eff} = echo spacing, 15; excitations, 1; readout bandwidth, ±32 kHz; field of view, 18 cm; matrix,= 64 × 64. Signal intensity measurements were made from square-shaped regions of interest with a fixed size of 8 × 8 pixels.

The null TI for each phantom was determined for echo train lengths of 4, 6, 8, 10, 12, 14, 16, 18, and 20 by using relatively small TI increments (2 milliseconds) and monitoring the signal intensity from the phantoms as it changed from negative to positive values. Plotting signal intensity versus TI, the null TI was determined by the intersection of the line joining the two consecutive TIs that cause a sign flip with the x-axis. These experiments were performed for a TR of 700, 1000, 2000, 4000, 6000, 10 000, and 20 000. Using data fitting based on a T1 relaxation formula, plots of null TI versus echo train length at different TRs were generated for both phantoms (Figs 1 and 2).

Phantom A was imaged using the above fixed parameters, a TR of 700 and a TI of 127 (determined null TI for phantom A at an echo train length of 4) while varying the echo train length from 4 to 16 by increments of four (Fig 3). Phantom B was imaged using the above fixed parameters, a TR/TI of 2000/800, and a TR/TI of 6000/1615, respectively (determined null TIs for phantom B at an echo train length of 4) while varying the echo train length from 4 to 16 by increments of four (Figs 4 and 5).

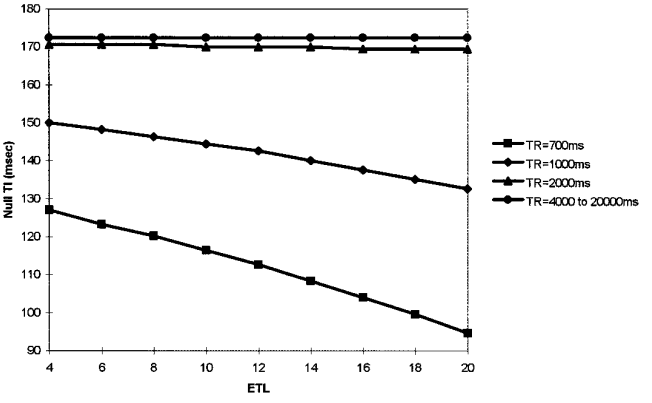

Fig 1. Plots of null TI for phantom A (corn oil) versus echo train length for different assigned TRs.

Volunteer Group

MR imaging of the cervical spine was performed in two healthy male volunteers (average age, 29 years) using a fast inversion-recovery sequence implementing the above-described hybrid RARE readout (TE_{eff} = echo spacing). The following parameters were used: TR/TE_{eff}/echo spacing/excitations, 1000/15/15/2; readout bandwidth, ±32 kHz; field of view, 18 cm (50% rectangular); matrix, 128 × 256. The null TI of bone marrow at an echo train length of 4 was determined by varying TI to achieve complete suppression of signal from the vertebral bodies of the cervical spine. Both volunteers were then reimaged at echo train lengths of 8 and 12 (Fig 6) with application of that null TI. The experiment was repeated with a TR of 4000 and an adjusted null TI of bone marrow at an echo train length of 4.

To study the effect of the hybrid RARE readout on fluid-attenuated inversion-recovery (FLAIR) sequences, a different echo-to-view mapping scheme was used. A linear (sequential) filling of k-space was implemented to adjust for the relatively long TE_{eff} (150 milliseconds) commonly used in clinical practice. With this echo-to-view mapping scheme, the echo spacing varies with changes in echo train length and does not equal TE_{eff}.

MR imaging of the brain was performed in two healthy male volunteers (average age, 34 years) using a fast inversion-recovery sequence implementing a linear hybrid RARE readout. The following parameters were used: 6000/150/2 (TR/TE_{eff}/excitations); readout bandwidth, ±32 kHz; field of view, 22 cm; matrix, 256 × 256. The null TI of CSF was determined at an echo train length of 16 and an echo spacing of 17 milliseconds (echo train length × echo spacing = 272 milliseconds). Using that null TI, both volunteers were then reimaged with an echo train length of 26 and an echo spacing of 11.6 milliseconds (echo train length × echo spacing = 300 milliseconds) (Figs 7 and 8).

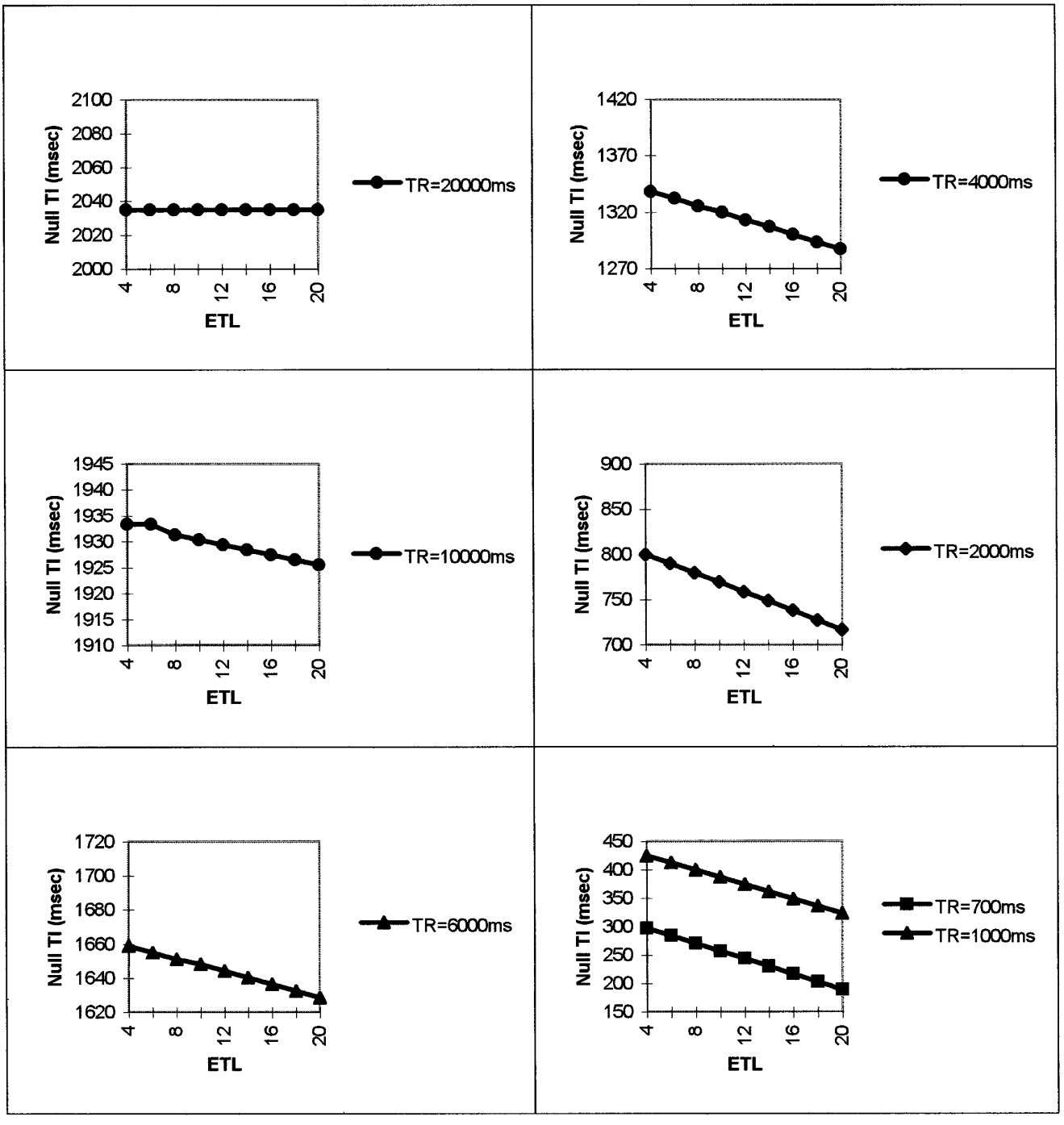

Fig 2. Plots of null TI for phantom B (water) versus echo train length for different assigned TRs.

Results

Phantom Experiments

Figure 1 presents plots of null TI for phantom A (corn oil) versus echo train length at different assigned TRs. There is a gradual decrease of null TI with echo train length up to a TR of 2000. At TRs of more than 2000, there is no change in the null TI as a function of the different echo train lengths used in this experiment. Also, the rate of decrease (absolute values of the slopes) in null TIs diminishes as TR increases from 700 to 2000.

Figure 2 presents plots of null TI for phantom B (distilled water) versus echo train length at different assigned TRs. There is a gradual de-

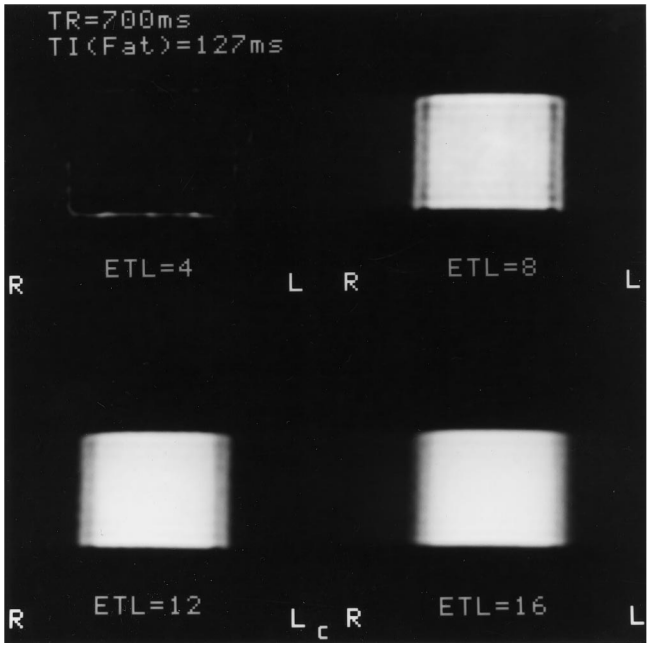

Fig 3. MR images of phantom A using a fixed TR/TI (700/127) and varying the echo train lengths (4, 8, 12, and 16). There is a gradual increase of signal (ie, loss of suppression) from the phantom with echo train length.

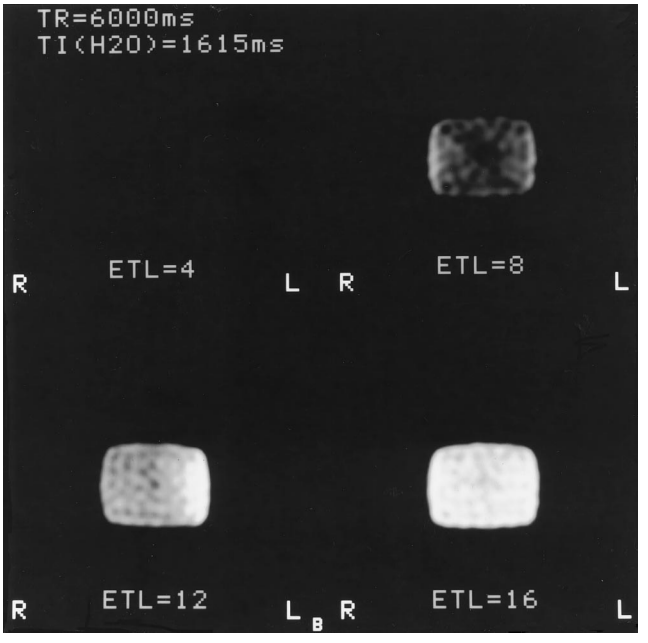

Fig 5. MR images of phantom B using a fixed TR/TI (6000/1615) and varying the echo train lengths (4, 8, 12, and 16). There is a gradual increase of signal (ie, loss of suppression) from the phantom with echo train length. Note that the rate of increase of signal from the phantom as a function of echo train length is more gradual at a TR of 6000 than at a TR of 2000 (Fig 4).

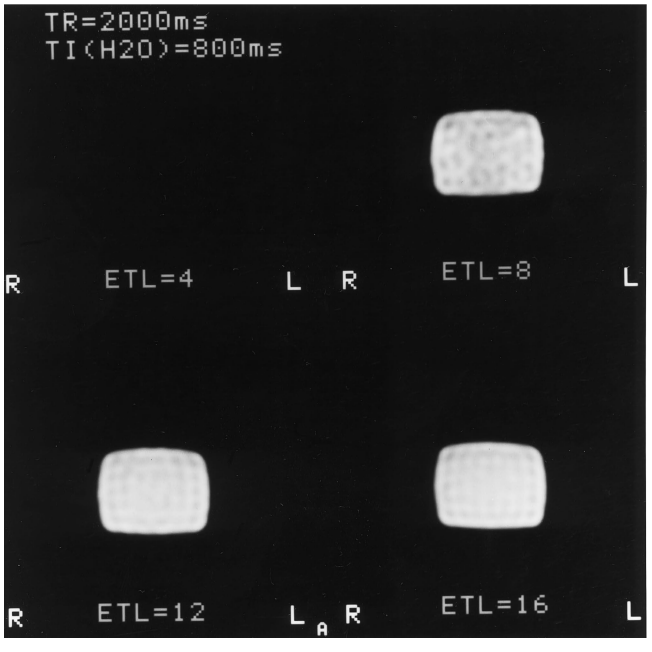

Fig 4. MR images of phantom B using a fixed TR/TI (2000/800) and varying the echo train lengths (4, 8, 12, and 16). There is a gradual increase of signal (ie, loss of suppression) from the phantom with echo train length.

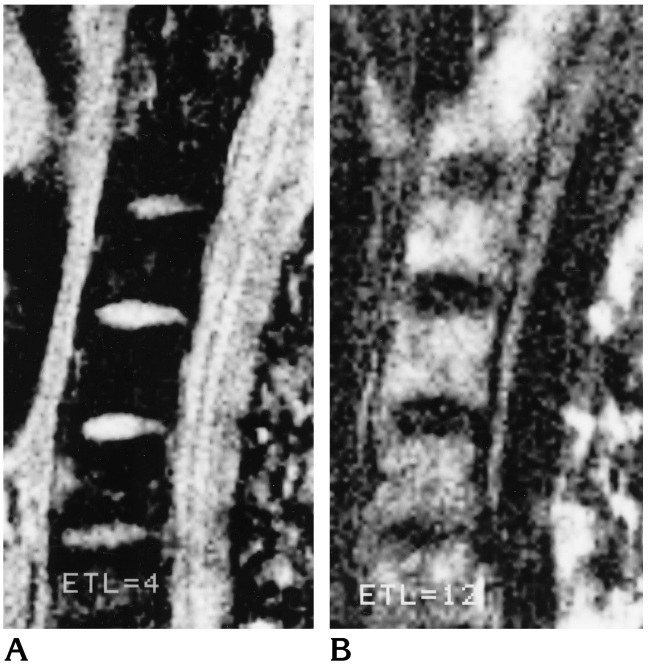

Fig 6. MR images of the cervical spine (1000/241/15, TR/TI/TE_{eff}) at echo train lengths of 4 (*A*) and 12 (*B*). There is a gradual appearance (ie, loss of suppression) of signal from the bone marrow of the cervical spine as the echo train length is increased.

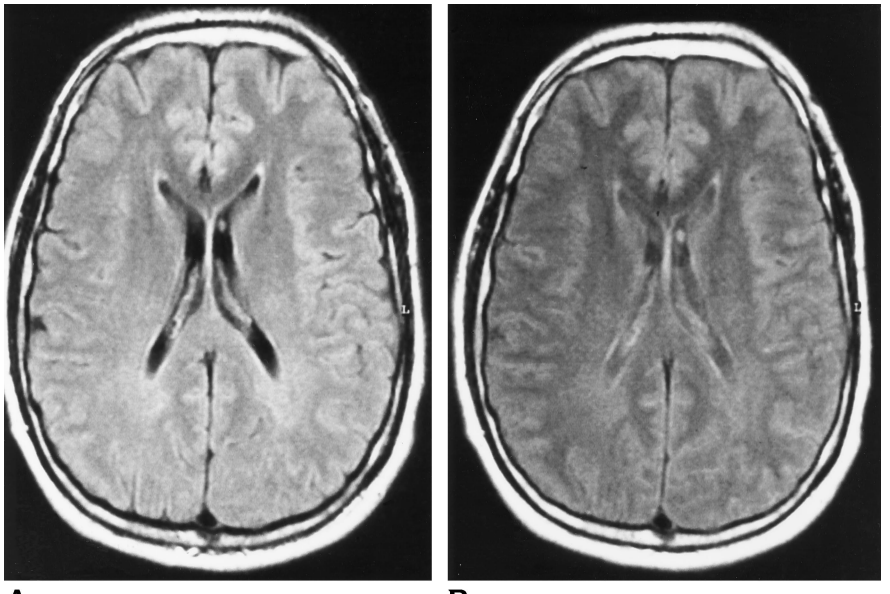

Fig 7. MR images of the brain (first volunteer) using a standard fast FLAIR pulse sequence (6000/2000/150). There is loss of adequate suppression of signal from CSF in the lateral ventricles as the product of the echo train length and echo spacing is increased from 272 milliseconds (*A*) to 300 milliseconds (*B*).

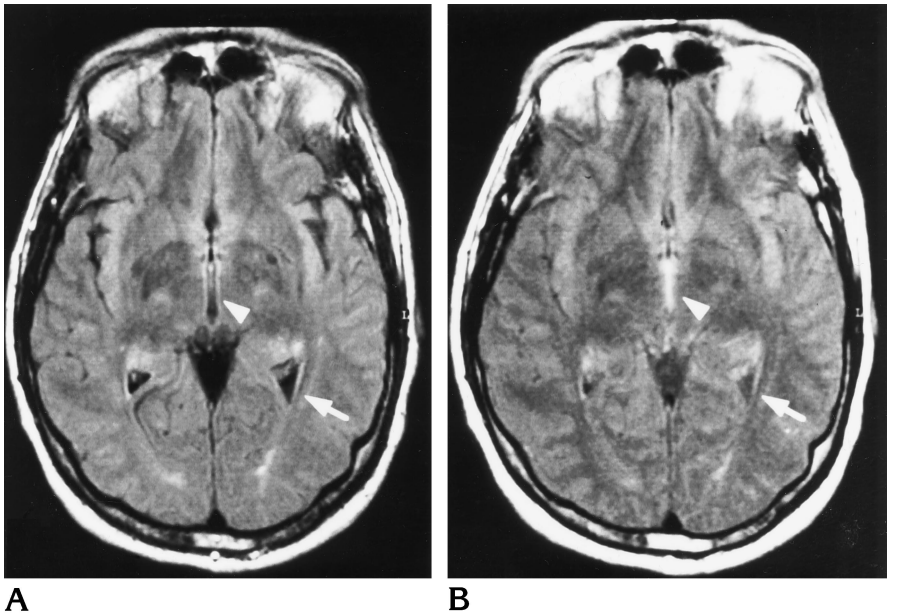

Fig 8. MR images of the brain (second volunteer) using a standard fast FLAIR pulse sequence (6000/2000/150). There is loss of adequate suppression of signal from CSF in the third ventricle (*arrowhead*) and trigone (*arrow*) as the product of the echo train length and echo spacing is increased from 272 milliseconds (*A*) to 300 milliseconds (*B*).

crease of null TI with echo train length up to a TR of 10 000. At a TR of 20 000, there is no change in the null TI as a function of the different echo train lengths used in this experiment. Also, the rate of decrease (absolute values of the slopes) diminishes as TR increases from 700 to 10 000.

Figure 3 demonstrates MR images of phantom A at a fixed TR/TI of 700/127 (determined null TI for phantom A at an echo train length of 4) and at different echo train lengths. At an echo train length of 4, there is an expected complete suppression of signal from the phantom. As the echo train length is increased by increments of four up to 16, there is loss of suppression and gradual signal increase from the phantom.

Figures 4 and 5 show phantom B at fixed TR/TIs of 2000/800 and 6000/1615, respectively (determined null TI for phantom B at an echo train length of 4) and at different echo train lengths. At an echo train length of 4, there is an expected complete suppression of signal from the phantom. As the echo train length is increased by increments of four up to 16, there is loss of suppression and gradual signal increase from the phantom. Note that the rate of signal

increase from the phantom as a function of echo train length is greater for a TR of 2000 than for a TR of 6000.

Volunteer Group

Figure 6 shows a gradual loss of suppression of signal from the cervical spine bone marrow as the echo train length increases from 4 to 12 at a fixed TR (1000), TI, and TE_{eff}. With a TR of 4000, complete suppression of signal from bone marrow is maintained despite increases in echo train length.

Figures 7 and 8 illustrate loss of adequate suppression of signal from CSF as the product of the echo train length and echo spacing is increased from 272 to 300 milliseconds.

Discussion

In the past, the clinical utility of inversion-recovery sequences has been limited by long acquisition times. The incorporation of a hybrid RARE readout to inversion-recovery MR pulse sequences has been instrumental in increasing their clinical usefulness (13).

Our results demonstrate a definite effect of the hybrid RARE readout on signal intensity and null TI of both fat (bone marrow) and water (CSF) for a specific range of TRs. The effect of the hybrid RARE readout on null TI of fat disappears at a much lower TR (4000) as compared with that of water (20 000) for the echo spacing and range of echo train lengths chosen in the phantom experiments (Figs 1 and 2).

One fundamental difference between conventional spin-echo and hybrid RARE readouts is the time allowed for postsampling signal recovery (15). For conventional spin-echo readouts, effective recovery of longitudinal magnetization begins immediately after the refocusing 180° radio-frequency pulse. For conventional inversion-recovery pulse sequences, the time allowed for postsampling signal recovery is approximately TR − TI − TE/2. The incorporation of a hybrid RARE readout allows effective recovery of longitudinal magnetization to begin after the last 180° radio-frequency pulse of the echo train, thus shortening the time allowed for postsampling signal recovery proportional to the product of echo train length and echo spacing. For fast inversion-recovery pulse sequences, the time allowed for postsampling signal recovery is approximately TR − TI − echo train length × echo spacing.

The recovery of longitudinal magnetization during a specific time period is dependent on the T1 relaxation of a particular tissue. If the time allowed for postsampling signal recovery is more than four to five times the T1 of a particular tissue, then complete recovery of longitudinal magnetization is expected. If, however, the time allowed for postsampling signal recovery is less than four to five times the T1 of a particular tissue, then incomplete recovery of longitudinal magnetization will occur, resulting in a new steady-state longitudinal magnetization. When coupling a hybrid RARE readout to an inversion-recovery pulse sequence, the magnitude of the steady-state longitudinal magnetization of a particular tissue will decrease as the product of echo train length and echo spacing increases, thus reducing its null TI.

We have found that shortening the TR results in a greater effect of echo train length on the time allowed for postsampling signal recovery and on the null TI. Owing to differences in the T1 relaxation of the two phantoms ($T1_{phantom\ A}$/$T1_{phantom\ B}$: 218 ± 5 milliseconds/3175 ± 70 milliseconds), complete recovery of longitudinal magnetization may be expected for phantom A at a much shorter TR than that for phantom B for the studied range of echo train lengths (Figs 1 and 2).

The hybrid RARE readout chosen for our phantom experiments implements an echo-to-view mapping scheme that maintains a constant echo spacing equal in value to the TE_{eff}. This enables the study of echo train length × echo spacing on the time allowed for postsampling signal recovery by varying the echo train length without accompanying changes in echo spacing.

Our choice of phantoms reflects an attempt to simulate tissues that are selectively suppressed in clinical practice; namely, fat and CSF (3–6). Further, the effects of magnetization transfer, amplified by hybrid RARE techniques, are negligible on signal intensity and on null TI of fat and CSF (16–18). On the other hand, for tissues susceptible to magnetization transfer effects (eg, white matter), further experimental and theoretical investigations are needed to define the various effects of the hybrid RARE readout on the generated signal and on the null TI.

Despite definite increases in signal intensity from both phantoms as a function of echo train

length (echo train length × echo spacing) at a fixed TR and TI (Figs 4–6), these increases may escape visual perception owing to the wide dynamic range of gray scale used in clinical imaging. Depending on the window and level used, increases in signal intensity from tissues may not necessitate a change in the assigned gray scale. In fast FLAIR MR imaging of the central nervous system, these increases in signal intensity from CSF may have to approach the signal intensity from brain before they are apparent. The heavy T2 weighting (TE_{eff}: 150 to 200) used in clinical imaging with fast FLAIR reduces the signal intensity from normal brain tissue (T2 decay) (5). This reduction renders the fast FLAIR MR images more susceptible to incomplete suppression of signal from CSF as a result of increases in the echo train length × echo spacing at a fixed TR and TI (Figs 7 and 8). Other causes of incomplete suppression of signal from CSF have been attributed to ghosting artifacts caused by inflow of nonnulled CSF into sections with high CSF flow rates (7). This lack of uniformity in signal suppression from CSF may limit the clinical utility of the fast FLAIR technique in the detection of acute subarachnoid hemorrhage and meningitis (8).

In conclusion, the hybrid RARE readout, commonly coupled to inversion-recovery MR pulse sequences in clinical use, has a definite effect on signal intensity and on null TI of tissues over a specific range of TRs. This effect is negligible when the time allowed for postsampling signal recovery exceeds four to five times the T1 relaxation time of a particular tissue (TR − TI − echo train length × echo spacing > 4 to 5 × T1) and, conversely, is amplified when the time allowed for postsampling signal recovery decreases below four to five times the T1 relaxation time. To optimize specific tissue suppression (eg, fat and CSF), radiologists implementing fast inversion-recovery MR imaging (fast short-TI inversion-recovery and fast FLAIR) should be aware of the effects of the hybrid RARE readout on null TI.

References

1. Bydder GM, Young IR. MR imaging: clinical use of the inversion recovery sequence. *J Comput Assist Tomogr* 1985;9:659–675
2. Bydder GM, Steiner RE, Blumgart RH, et al. MR imaging of the liver using short TI inversion recovery sequence. *J Comput Assist Tomogr* 1985;9:1084–1089
3. Dwyer AJ, Frank JA, Sank VJ, et al. Short T1 inversion recovery sequence: analysis and initial experience in cancer imaging. *Radiology* 1988;168:827–836
4. Atlas SW, Grossman RI, Hackney DB, et al. STIR MR imaging of the orbit. *AJNR Am J Neuroradiol* 1988;9:969
5. Hajnal JV, Bryant DJ, Kasuboski L, et al. Use of fluid-attenuated inversion recovery (FLAIR) pulse sequences in MRI of the brain. *J Comput Assist Tomogr* 1992;16:841–844
6. White SJ, Hajnal JV, Young IR, et al. Use of fluid-attenuated inversion recovery pulse sequences for imaging the spinal cord. *Magn Reson Med* 1992;28:153–162
7. De Coene B, Hajnal JV, Gatehouse P, et al. MR of the brain using fluid-attenuated inversion recovery (FLAIR) pulse sequences. *AJNR Am J Neuroradiol* 1992;13:1555–1564
8. Noguchi K, Ogawa T, Inugami A, et al. Acute subarachnoid hemorrhage: MR imaging with fluid-attenuated inversion recovery pulse sequences. *Radiology* 1995;196:773–777
9. Park HW, Cho MH, Cho ZH. Time-multiplexed multi-slice inversion-recovery techniques for NMR imaging. *Magn Reson Med* 1985;2:534–539
10. Stehling MK, Ordidge RJ, Coxon R, et al. Inversion-recovery echo-planar imaging (IR-EPI) at 0.5 T. *Magn Reson Med* 1990; 13:514–517
11. Rydberg JN, Hammond CA, Grimm RC, et al. Initial clinical experience in MR imaging of the brain with a fast fluid attenuated inversion-recovery pulse sequence. *Radiology* 1994;193: 173–180
12. Rydberg JN, Riederer SJ, Rydberg CH, et al. Contrast optimization of fluid-attenuated inversion recovery (FLAIR) imaging. *Magn Reson Med* 1995;34:868–877
13. Hashemi RH, Bradley WG, Dar-Yeong C, et al. Suspected multiple sclerosis: MR imaging with a thin-section fast FLAIR pulse sequence. *Radiology* 1995;196:505–510
14. In den Kleef JJE, Cuppen JJM. RLSQ: T1, T2 and rho calculations, combining ratio's and least squares. *Magn Reson Med* 1987;5:513–524
15. Lee JN, Riederer SJ. A modified saturation-recovery approximation for multiple spin-echo pulse sequences. *Magn Reson Med* 1986;3:132–134
16. Wolff SD, Balaban RS. Magnetization transfer contrast (MTC) and tissue water proton relaxation in vivo. *Magn Reson Med* 1989;10: 135–144
17. Eng J, Ceckler TL, Balaban R. Quantitative ^1H magnetization transfer in vivo. *Magn Reson Med* 1991;17:304–314
18. Melki PS, Mulkern RV. Magnetization transfer effects in multislice RARE sequences. *Magn Reson Med* 1992;24:189–195